



GLOBAL JOURNAL OF RESEARCHES IN ENGINEERING: A
MECHANICAL AND MECHANICS ENGINEERING
Volume 23 Issue 4 Version 1.0 Year 2023
Type: Double Blind Peer Reviewed International Research Journal
Publisher: Global Journals
Online ISSN: 2249-4596 & Print ISSN: 0975-5861

Preliminary Prototyping and Simulations to Explore Mechanical Properties of 3D Printed Materials for Supporting the Head

By Matthew Dickinson

Abstract- A novel exoskeleton design has been produced that assists the contraction of neck muscles. 3D printing has been employed to reduce costs of manufacturer. The two printing materials employed were Polylactic acid (PLA) and polyethylene terephthalate with carbon (PET-C), and the central spinal cord of the design being Nitrile rubber. The aim of this work was to study the use of 3D printed materials as the main skeletal structure to support the human head and neck. To identify if the 3D printable materials could be offered as an equivalent alternative to conventional more expensive materials. A simulation and proto type were created for this work. An exoskeleton was designed to assist with neck extension. A maximum load of lift force was calculated to be 20N, and this was incrementally reduced to study the effects on the material. A total number of 10 simulations were run to study the head in conditions with no muscular support through to 90% of operational support. When measured against the head, the material performed well within its operational value.

Keywords: 3D printing, exo-skeleton, PLA, PETC.

GJRE-A Classification: DDC Code: 519.2 LCC Code: QA273



PRELIMINARY PROTOTYPING AND SIMULATIONS TO EXPLORE MECHANICAL PROPERTIES OF 3D PRINTED MATERIALS FOR SUPPORTING THE HEAD

Strictly as per the compliance and regulations of:



RESEARCH | DIVERSITY | ETHICS

© 2023. Matthew Dickinson. This research/review article is distributed under the terms of the Attribution-NonCommercial-No Derivatives 4.0 International (CC BY-NC-ND 4.0). You must give appropriate credit to authors and reference this article if parts of the article are reproduced in any manner. Applicable licensing terms are at <https://creativecommons.org/licenses/by-nc-nd/4.0/>.

Preliminary Prototyping and Simulations to Explore Mechanical Properties of 3D Printed Materials for Supporting the Head

Matthew Dickinson

Abstract- A novel exoskeleton design has been produced that assists the contraction of neck muscles. 3D printing has been employed to reduce costs of manufacturer. The two printing materials employed were Polylactic acid (PLA) and polyethylene terephthalate with carbon (PET-C), and the central spinal cord of the design being Nitrile rubber. The aim of this work was to study the use of 3D printed materials as the main skeletal structure to support the human head and neck. To identify if the 3D printable materials could be offered as an equivalent alternative to conventional more expensive materials. A simulation and proto type were created for this work. An exoskeleton was designed to assist with neck extension. A maximum load of lift force was calculated to be 20N, and this was incrementally reduced to study the effects on the material. A total number of 10 simulations were run to study the head in conditions with no muscular support through to 90% of operational support. When measured against the head, the material performed well within its operational value. The validation of this work showed a m difference which could have been related to the ability of the material to combine while being manufactured. This study presents work in the form of a novel exoskeleton that presents 3D printing as a possible alternative to conventional manufacturing.

Keywords: 3D printing, exo-skeleton, PLA, PETC.

I. INTRODUCTION

Over the past decade the development of wearable robotic structures for replacement limbs for rehabilitation's has received attention by many researchers and developers. [1–7] Exoskeleton systems have been traditionally designed for the 1 manufacturing and military sectors, prioritising the ability to move a large mass as efficiently as possible. [8, 9] These systems primarily support an able person's lower body to assist in difficult tasks, such as carrying a load whilst navigating tough terrain, of which the human body alone would not be capable. One example of this type of development is the Berkeley Lower Extremity Exoskeleton (BLEEX) which was designed for applications where a wheeled vehicular transport is not practical. [10] In the past decade, with motors reducing in size and advancements in battery technology, there has been an increase in exoskeleton development for medical purposes. There are two main types of exoskeleton in this category; rehabilitative exoskeletons and assistive exoskeletons. Rehabilitative examples aim

to assist with the recovery of total or partial motor abilities. These systems are designed to be reusable, but temporary solution for those patients who have suffered, or are suffering from, a curable illness or injury. Assistive exoskeletons are used for patients who have a permanent disability, such as an amputated limb, or a muscular degenerative disease. Both of these systems can greatly improve quality of life. Spinal cord injuries (SCI) are one of the most common reasons for paralysis. In 2010, Berkeley Bionics unveiled their latest exoskeleton development "eLEGS". This system allowed users who suffer with mobility disorders, or are paralysed, to stand and walk. This light weight (20.4 kg), lower limb exoskeleton structure allows wearers to walk upright with little physical exertion. To control the system, the user's intent is measured and this is then passed through a proportional–integral–derivative (PID) feedback-loop found on a micro controller. The output signal is then used to drive the motors in the system thus facilitating movement. [11] Dynamically driving a machine that will assist it the actuation of the human body is an extremely complicated problem. [12–14] Ensuring that muscles are helped to move, using a similar pattern to the human central pattern generator (CPG), [15] and ensuring that the system is lightweight and simple to use, prove to be some of the largest challenges in creating devices of this nature. A team at Columbia Engineering developed a Robotic Spine Exoskeleton (RoSE), designed to assist patients with spinal abnormalities. [3] Spinal deformities are usually treated by using a fixed brace around the torso and hips to correct the abnormality. [16] Studies showed that the device allows for the three dimensional forces of the human torso to be mapped via force and position sensors mounted to the actuators, allowing for control methodology known as impedance, which is a method of control which simply regulates the position or force of a system. The RoSE, consists of three rings placed on the pelvis, mid-thorax, and upper-thorax. These rings are connected by 6 pairs of motors to produce a total of 12 degrees of freedom. By using a PID controller, the system can apply corrective forces in any direction, focussing on specific areas of the spine whilst also having freedom of movement in ways which do not affect it. [3] Since the early 1980's when Charles Hull introduced the world first 3D printer, 3D printing has

Author: e:mail- mdickinson1@uclan.ac.uk

become a major interest in the research and development environment. [17] These machines have become widely available due the massive reduction in cost and increased availability of low cost technology. With the development of high performing source materials, researchers have begun use of 3D printed materials for orthotic and prosthetic 2 applications. [18–20] Zuniga presented a study that examined the use of Polylactic acid (PLA) as a material for manufacturing of low cost prosthetic limbs. The study successfully demonstrated the use of PLA for the manufacture of prosthesis could serve as an alternative to conventional high priced material, however, the conclusions did highlight a problem in that PLA has poor thermal performance and noted that fluctuations in heat can lead to components failure. [21] In an effort to address the low thermal performance of the material Bo-Hsin presented an improved PLA filament by modifying the –NCO (Cyanate) and the –OH (Hydroxide) ratio of the material, resulting in glass transition temperature (Tg) improvement from the standard 55oC to 64oC. [22] With these advancements further development into the use of 3D printed materials within the medical world have been untaken, more specifically single limb orthoses and upper limb prostheses. [23] By the use of 3D printing the manufacturing of components, the exoskeleton has the potential to offer an improved quality of life for millions of people around the world. The use of exoskeleton technology is in it’s infancy with the problems of accessibility preside, at present the costs of these devices can be as high as \$45,000 per system. [24] Offering these types of technology’s to low income countries can prove to be extremely difficult. One possible way of lowering the price of these skeletons is to consider the costs for manufacturing and ease of maintenance, by incorporating the use of 3D printing technologies. Typically exoskeletons are made from rigid, structured materials such as aluminium. [5, 25–28] Recently, 3D printing has proven to be a tool that has the potential to impact the field of prostheses and orthoses. [20, 29] Similar to traditional methods, the use

of 3D printing allows the designer to offer a tailored fit to the patient’s limb or amputated area. 3D-printed objects can be made from Polylactic acid (PLA), which is a cheap and strong alternative to a traditional material, such as Aluminium. [30] This paper presents the use of 3D printed materials for exoskeleton structures. The work forms part of a larger exoskeleton project that we have named “E’ssist”.

II. DESIGN

The initial design challenge for the exoskeleton was to develop an actuating system that assist in the extension of the neck. The system has been designed to be used in conjunction with a neck support wrap. Two Actuonix linear actuators where used to provide alternative to the typical muscle strength, each motor was attached to a connector which in turn provided the assistive moment to the head. The position of the connectors were deemed one of the most important elements of the prototype exoskeleton, as wrongly positioned actuation points could lead to further muscle damage and/or injury to the subject. The trigger points of the trapezius muscle were used as key areas for actuation. Work noted by Palastanga confirmed the muscle is the main point of head support for mobility. [31] The exoskeleton under development is predominantly aimed at children with muscular deficiencies, and therefore a user height range of 100 cm 3 to 180 cm was chosen and the system was designed accordingly. The strength range that influenced motor selection was based on a study by Hosking, where 19 children aged between 4 and 13 years of age were subject to a series of strength tests. [32] In this work, only the upper trapezius muscles were assessed through “Neck Flexor” examinations. Further work from Sandercock confirmed these examinations remain relevant. [33] A study completed by Villia explicitly examined skeletal muscle function in children, at the age of 11 years 33. The results from both studies agreed, and they are listed in Table 1.

Table 1: Neck Muscle Strength

Muscle Group	Min (height = 100 cm)	Max (height = 170 cm)
Trapezius	20 N	80 N

To verify the Trapezius results noted in these studies, the human head force (HF) was modelled as a Class 1 lever. The centre of gravity (CG) relative to the pivot point around the atlas vertebra acts at a displacement of roughly half of the force lever arm.

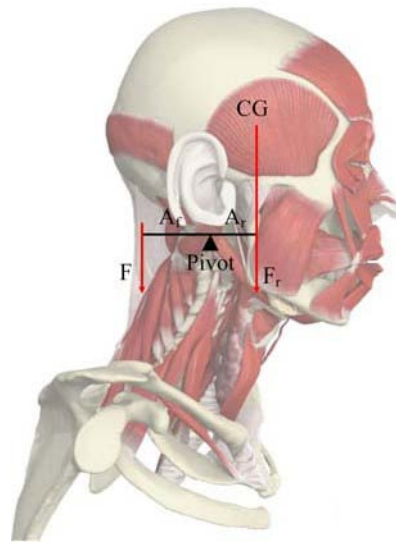


Figure 1: First Class Lever Human Head

Figure 1 shows the human head, for which a Class 1 lever is assumed to be an appropriate model, where A_r , A_f , F_r and F are the resistance arm, the force arm or the lever, resistance force of the human head and force generated by the muscle to operate the lever, respectively. Palastanga [31] suggests that the force and the resistance arms are directly related to each other, thus the resistance arm of the lever is calculated as:

$$A_r = \frac{A_f}{2} \quad (1)$$

Where A_f and A_r is the distance from the atlas vertebra to the point of muscular interface and resistance arm, respectively. The mass of the head is assumed to be in the range 4 kg - 5 kg.

$$H_F = \frac{F_r A_r}{A_f} \quad (2)$$

Based on this, a pair of linear actuators were used to share the loading of H_F . The motors performance rating is noted in Table 2.

Table 2: Linear Actuator

Motor	Force (N)	Key point muscle group area
L12 Micro Linear Actuator	42N	Trapezius

Table 3: Material Masses

Compnents	Material	Mass (g)
Top Segment	PLA	54.1
Middle Segment	PLA	26.6
Bottom segment	PLA	68.6
Connectors x 4	PET-C	14
Actuators x 2		56
Total mass		317.3

The design of the structure is shown in Figure 3.

To enable smooth transition from the force delivered from the motor through to the body, a novel connection method was proposed Figure 2.

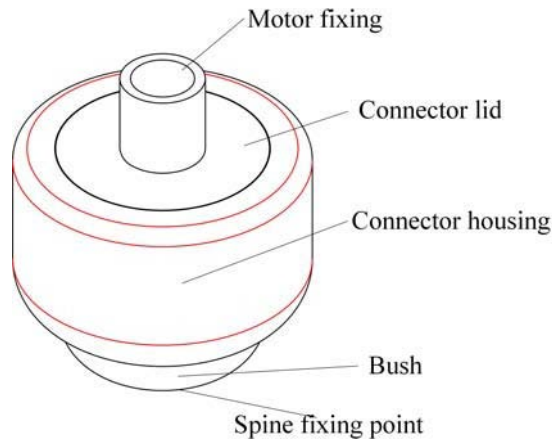


Figure 2: Connector Assembly

The connector ensured that the muscle did not receive direct force from the motor as this may cause damage to the subject (Figure 6). This also added a three degrees of freedom relationship between the spine segment and the linear actuator connecting point. Both connector lid and housing were made from a

Polyethylene terephthalate with carbon mixture (PET-C). These components were 3D printed with 40 % infill of material with a triangular support structure. Both the bush and the central cords were Nitrile rubber (NBR).

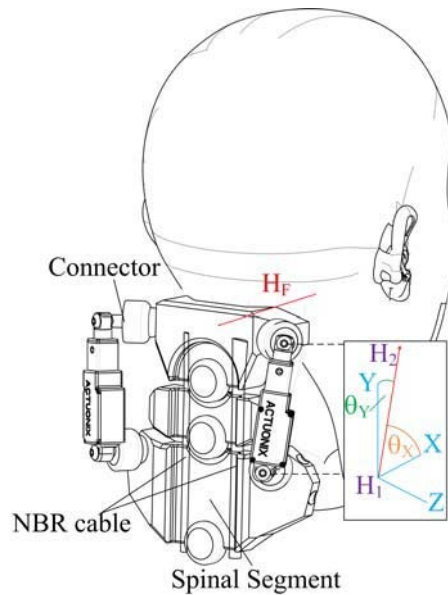


Figure 3: Neck Exo-Structure

By taking the precise locations for H_1 and H_2 which are the coordinate locations of where the actuators connect respectively, it was possible to calculate the vectors, representative of the actuation during operation, as follows:

$$F_x = 42N \sin \theta_x \quad (3)$$

$$F_y = 42N \sin \theta_y \quad (4)$$

Where F_x and F_y are the vector force for both x and y components respectively. The maximum output from the actuators used is 42 N and where ϑ_x and ϑ_y are the directional vector angles in respects to H_1 and H_2 . To

consider the variation in neck muscular assistance, the simulations were run with a variation of H_f . 2 N assumes that 90% of the muscles are actively supporting the mass of the head and at 20 N it was assumed that there was no muscular assistance, hence all support drive was provided by the exoskeleton. From the minimum value Increments of 10% in H_f were studied. As noted by Abbot, when simulating 3D printed materials it is good practice to verify the material used within the simulation. [34] To verify the material values used within the simulation the deformation and stress concentration were calculated using the deflection of a cantilever. This is represented as:

were calculated using the deflection of a cantilever. This is represented as:

$$y = \frac{PL^3}{3EI} \quad (5)$$

Where y , P , L , E and I are the maximum deflection, load, length, modulus of elasticity and moment of inertia, respectively.

$$\sigma_{bend} = \frac{Py}{I} \quad (6)$$

Where λ_1 , λ_2 and λ_3 are the distortional principal stretches of the material. ω is the strain energy function, J_{el} is the elastic ratio of the material, μ_k , α_k and β_k are functions of the material properties. When simulating the hyper elastic material in an FE package, these parameters need to be provided as an input, and the values used in this work are taken from. [37] As the notation of the bush on the connector is subject to

$$\Psi(C_{10}, C_{01}, \kappa) = C_{10}(I_1^* - 3) + C_{01}(I_2^* - 3) + \frac{\kappa}{2}(J - 1)^2 \quad (8)$$

As noted in equation 8, the nearly incompressible Mooney-Rivlin method operates with three key properties of the material. C_{10} is the representation of elastic behaviour of the material, C_{01} this is the none linearity component of the material, and κ is the bulk modulus. Showing the connection between Stokers and Mooney in $I_n = \lambda^2 + \lambda^2 + \lambda^2$. To ensure our results remained accurate, the 3D printed components were modelled in Autodesk Inventor with an internal geometry representative of the infill structure.

The test equipment was produced on an Ultimaker S5, both the connector and spine segments

Both equations were applied in a simple bending test to verify the material data being used in the simulation. As the spinal structure is connected with NBR cords, hyper elastic phenomena will occur during this operation. One of the most popular models for the extension of elastic material is Storakers equation [35], more specifically for this work the Ogden model was used [36], which operates by the materials strain energy function:

$$\omega = \sum_{k=1}^N \frac{2\mu_k}{\alpha_k} \left[\lambda_1^{\alpha_k} + \lambda_2^{\alpha_k} + \lambda_3^{\alpha_k} - 3 + \frac{1}{\beta_k} \left(J_{el}^{-\alpha_k \beta_k} - 1 \right) \right] \quad (7)$$

rotational strain, we used the Mooney-Rivlin two parameter model, as this model great shear behaviour. [38] The Mooney-Rivlin model is commonly seen as an extension to the to the Neo-Hookean model, by providing a greater accuracy on the elastic strain coefficient I_2^* variable by incorporating the use of the Helmholtz free energy per unit reference.

were produced with a 0.4 mm extruder head and 0.1 mm layer thickness. The 6 mm NBR cord was purchased and cut to size. Each connector was attached to the spine using a NBR bush Figure 4. The assembly was controlled through an Arduinouno and coded to cycle to maximum extension and maximum contraction. All cycles were run at 0 – 3 seconds. At the connection point between the segment and the connector a BF350 strain gauge was placed.

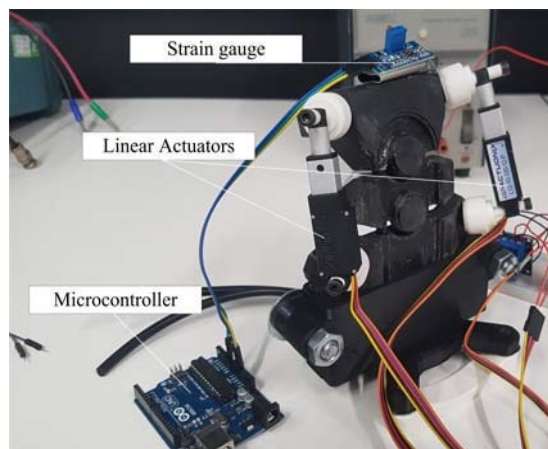


Figure 4: Neck Spine test Equipment

III. RESULTS

Simulation of the neck assembly was performed with COMSOL Multiphysics and validated with

experimental data using BF350 strain gauge and Arduino Uno on the linear actuator connector. Von Mises Stress are calculated because this is a way of testing to failure of the material.

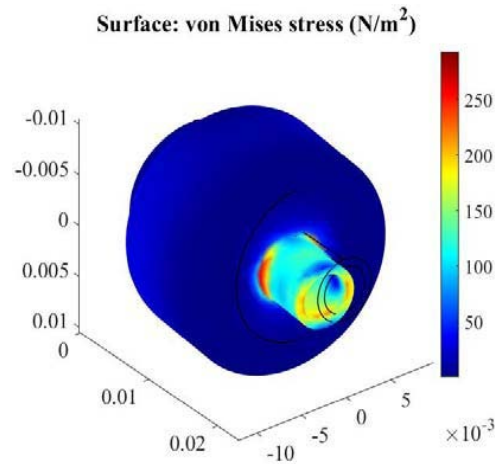


Figure 5: Connect Force Distribution

Figure 5 shows the connector after running the test at the maximum loading of 42 N. The resulting deformation and surface stress shows a maximum of 250.9 N/m² at the point of actuator connection and also

shearing force around the Nitrile interface. As the linear actuators are assumed to be in maximum operation, these results have been applied to the spinal segments in the simulation of all head force variations.

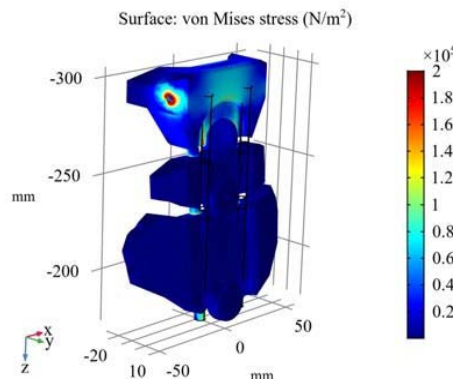


Figure 6: Neck Assembly with 42 N Linear Force

Figure 6 shows the neck in an isometric view aimed at the front and the rear of the assembly. The top segment that interfaces with the head and spine connection shows the most concentrated area of stress. This is located in particular around the NBR connections and the linear actuator interfaces. The maximum stress

is noted to be 2×10^5 N/m² which remains well within the Young's modulus of both PLA and the nitrile. Further testing was run to examine the neck assembly in variant conditions simulating situations where a subject would be capable of offering differing degrees of self-actuation of neck muscles.

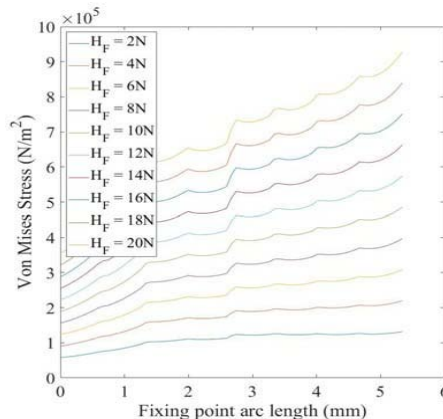


Figure 7: Neck Stress around Mounting Hole

Figure 7 shows the results from the simulation when varying the head force in the range of 2 – 20 N. When the H_f is tested at 20 N this assumes no assistance from muscular support, hence the

exoskeleton is holding the full weight of the head. The results from the simulation show that the exo-skeletal structure receives below $9.5 \times 10^5 \text{ N/m}^2$ of stress.

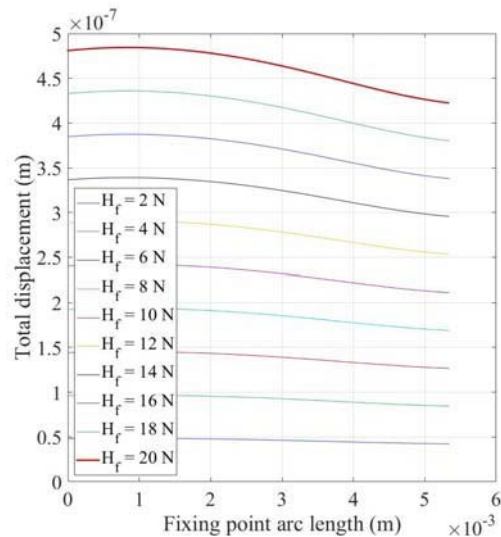


Figure 8: Top Joint Displacement

Figure 8 shows the displacement of the top joint after the range of H_f being applied. This showing that when maximum H_f is applied at 20 N the maximum

deformation of the joint is $480 \mu\text{m}$ and demonstrating a linear relationship between H_f and displacement.

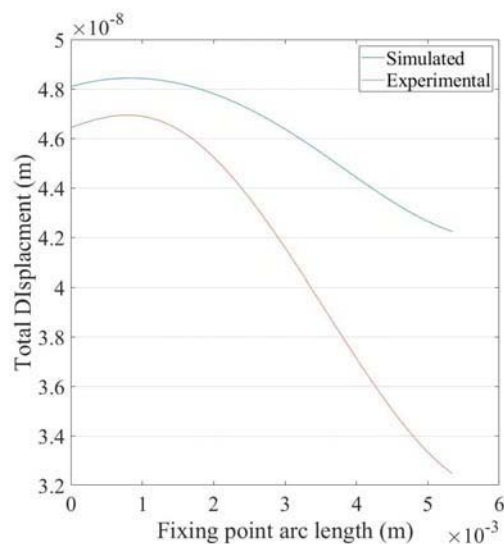


Figure 9: Simulated Vs Experimental Result

Figure 9 shows the results from the physical test equipment and also the simulation at head force of 2N. The simulation deformation begins at $4.8 \times 10^{-8} \text{ m}$ and ends above $4.2 \times 10^{-8} \text{ m}$, the physical results show above $4.6 \times 10^{-8} \text{ m}$ and ends above $3.2 \times 10^{-8} \text{ m}$, showing $1 \times 10^{-8} \text{ m}$ difference between both outputs.

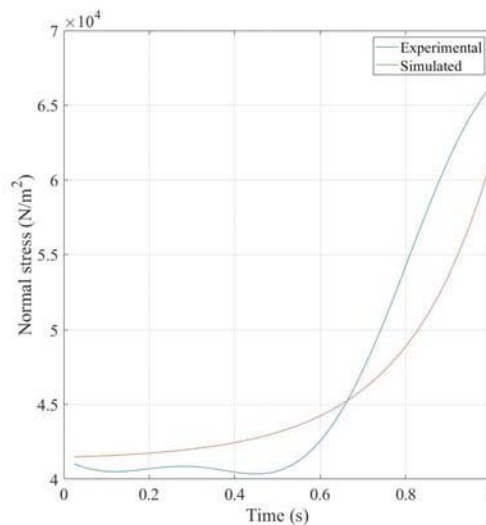


Figure 10: Caption

Figure 10 shows the results from the physical and simulated test result of H_f of 2N. The simulated stress begins 4.2×10^4 N/m² of force and ends above 6×10^4 N/m². The experimental results beneath 4.2×10^4 N/m² and end above 6.5×10^4 N/m², showing almost a 0.5 N/m² difference between the two results.

IV. DISCUSSION

In all simulations and experiments, the linear motors were actuated to their maximum displacement of 10 mm resulting in an arc length of the upper edge of the top segment of 5 mm. A resistance force representing the assistance or lack of assistance from a subject was varied between 2-20 N, and the resulting surface stress was simulated, firstly within the connector with an actuator force directly applied and secondly as part of a complete assembly of the neck prototype. As the connector was produced using PET (Carbon) the 250 N/m² stress exhibited are well below the yield stress of 2.7 GPa published for this material. [39] The stress predicted within the Nitrile rubber bush are also well within the tolerable limits published for this material. The results from the assembly simulation demonstrate the largest stress concentration are found in the upper segment where the mass of the subject's head would be supported. The concentrated forces in this segment result in stresses as high as 2×10^5 N/m² but once again, these lie well within the published yield stresses of PLA. Head force variation applied at 2N increments of resistance force, which assumes minimal assistance to the patient, the result demonstrate a linear relationship between deflection and Head Force $480\mu\text{m} - 48\mu\text{m}$, however a linear relationship between max stress and HF is not observed directly only through calculation of 13 rate of change of H_f with respect to stress is a linearity observed. To validate the results from the neck exoskeleton, the system was manufactured and run in the same conditions. The linear actuators were moved

by the full 10 mm and a resistance force was placed on to the neck of 2 N. When compared against the simulation results the initial starting displacement shows almost over 0.166×10^{-8} m difference between the simulated material and the manufactured material. The elastication of the material also shows a greater displacement than what is seen in the simulation, noting a difference of 0.976×10^{-8} m. The normal stress between the simulated and the manufactured material showed a maximum of 10% difference. As the material used within the simulation has been selected based on values presented within the COMSOL software, the variation of results could be an indicator that the PLA used has a slight greater performance as the one presented within the software. The experimental results show good corroboration with those from COMSOL simulation, error is deemed acceptable. The double nitrile lines which continue up the spine hold similar stress concentration to what is seen within the top section of the spine however, the patient will be unable to perform all ranges of motion, as head tilt is unachievable.

V. CONCLUSION

This study examines the use of 3D printed materials for use in wearable robotic structures. The human neck is a complex series of connected segments which work together to create a system that allows for 6 degrees of freedom (DoF). To ease the process of design this study has focused on the pitch element of human head motion (looking up and down). This study has demonstrated that 3D printed structures are suitable for use with exoskeleton components and the materials chosen here for this prototype design are able to meet the physical demands expected during operation. Additionally, these results have also demonstrated this prototype design is over engineered while at the same time providing a suitable method of refining design to

reduce materials used and maintain crucial structural integrity.

VI. FURTHER WORK

To further this work testing of the raw material to produce a detailed mechanical data base is recommended. With information of this nature the error difference between modelled and tested would become less. As the material is show to be able to support the body for assistive movement it is suggested that this work be continued to the lower spine section to examine the use of the structure on the torso area. Further to the design it is suggested that the dual nitrile lines be revised to a design which contains a single feed as full mobility of the neck and head could not be achieved in this solution.

Author Contributions

All authors contributed equally in the preparation of this article.

Declaration of Conflicting Interests

The author(s) declared no potential conflicts of interest with respect to the research, authorship, and/or publication of this article.

Funding

This work in this paper was funded entirely by the University of Central Lancashire.

REFERENCES RÉFÉRENCES REFERENCIAS

1. R. LeMoyné, *Advances for Prosthetic Technology: From Historical Perspective to Current Status to Future Application*. Springer Japan. [Online]. Available: <https://books.google.co.uk/books?id=F9G9CwAAQBAJ>.
2. M. M. Rodgers, G. Alon, V. M. Pai, and R. S. Conroy, "Wearable technologies for active living and rehabilitation: Current research challenges and future opportunities," vol. 6, pp. 1–9. [Online]. Available: <https://doi.org/10.1177/2055668319839607>.
3. J.-H. Park, P. R. Stegall, D. P. Roye, and S. K. Agrawal, "Robotic spine exoskeleton (RoSE): Characterizing the 3-d stiffness of the human torso in the treatment of spine deformity," vol. 26, no. 5, pp. 1026–1035.
4. M. J. Fu, M. Y. Harley, T. Hisel, R. Busch, R. Wilson, J. Chae, and J. S. Knutson, "Ability of people with post-stroke hemiplegia to self-administer FES-assisted hand therapy video games at home: An exploratory case series," vol. 6. [Online]. Available: <https://doi.org/10.1177/2055668319854000>.
5. L. E. Miller, A. K. Zimmermann, and W. G. Herbert, "Clinical effectiveness and safety of powered exoskeleton-assisted walking in patients with spinal cord injury: systematic review with meta-analysis," vol. 9, p. 455. [Online]. Available: <https://www.ncbi.nlm.nih.gov/pmc/articles/PMC4809334/>
6. P. Asselin, S. Knezevic, S. Kornfeld, C. Cimigliaro, I. AgranovaBreyter, W. A. Bauman, and A. M. Spungen, "Heart rate and 15 oxygen demand of powered exoskeleton-assisted walking in persons with paraplegia," vol. 52, no. 2, pp. 147–158. [Online]. Available: <http://www.rehab.research.va.gov/jour/2015/522/pdf/JRRD-2014-02-0060.pdf>
7. S. Federici, F. Meloni, M. Bracalenti, and M. L. De Filippis, "The effectiveness of powered, active lower limb exoskeletons in neurorehabilitation: A systematic review," vol. 37, no. 3, pp. 321–340. [Online]. Available: <https://content.iospress.com/articles/neurorehabilitation/nre1265>.
8. S. Karlin, "Raiding iron man's closet [geek life]," vol. 48, no. 8, pp. 25–25.
9. K. L. Mudie, A. C. Boynton, T. Karakolis, M. P. O'Donovan, G. B. Kanagaki, H. P. Crowell, R. K. Begg, M. E. LaFiandra, and D. C. Billing, "Consensus paper on testing and evaluation of military exoskeletons for the dismounted combatant," vol. 21, no. 11, pp. 1154–1161. [Online]. Available: <http://www.sciencedirect.com/science/article/pii/S1440244018301683>.
10. R. Steger, Sung Hoon Kim, and H. Kazerooni, "Control scheme and networked control architecture for the berkeley lower extremity exoskeleton (BLEEX)," in *Proceedings 2006 IEEE International Conference on Robotics and Automation, 2006. ICRA 2006*. IEEE, pp. 3469–3476. [Online]. Available: <http://ieeexplore.ieee.org/document/1642232/>
11. A. Zoss, H. Kazerooni, and A. Chu, "Biomechanical design of the berkeley lower extremity exoskeleton (BLEEX)," vol. 11, no. 2, pp. 128–138.
12. D. Zhang, V. Dubey, W. Yu, and K. H. Low, *Biomechatronics: Harmonizing Mechatronic Systems with Human Beings*. Frontiers Media SA, google-BooksID: inmGDwAAQBAJ.
13. *Anatomy and human movement - 7th edition*. [Online]. Available: <https://www.elsevier.com/books/anatomy-and-humanmovement/soames/978-0-7020-7226-0>.
14. R. P. McCall, *Physics of the Human Body*. JHU Press, google-Books-ID: LSyC41h6CG8C.
15. K. Minassian, U. S. Hofstoetter, F. Dzeladini, P. A. Guertin, and A. Ijspeert, "The human central pattern generator for locomotion: Does it exist and contribute to walking?" vol. 23, no. 6, pp. 649–663.
16. J. McAviney, J. Mee, A. Fazalbhoy, J. Du Plessis, and B. T. Brown, "A systematic literature review of spinal brace/orthosis treatment for adults with scoliosis between 1967 and 2018: clinical outcomes and harms data," vol. 21, no. 1, p. 87. [Online]. Available: <https://doi.org/10.1186/s12891-020-3095-x>.

17. C. W. Hull, "Apparatus for production of three-dimensional objects by stereolithography," U.S. Patent 1 4575330A, 1986-03-11. 16.
18. E. Wojciechowski, A. Y. Chang, D. Balassone, J. Ford, T. L. Cheng, D. Little, M. P. Menezes, S. Hogan, and J. Burns, "Feasibility of designing, manufacturing and delivering 3d printed ankle-foot orthoses: a systematic review," vol. 12, no. 1, p. 11. [Online]. Available: <https://doi.org/10.1186/s13047-019-0321-6>.
19. J. Fu, J. Liu, Y. Wang, B. Deng, Y. Yang, R. Feng, and J. Yang, "A comparative study on various turbocharging approaches based on IC engine exhaust gas energy recovery," vol. 113, pp. 248–257. [Online]. Available: <http://www.sciencedirect.com/science/article/pii/S0306261913005898>.
20. A. Manero, P. Smith, J. Sparkman, M. Dombrowski, D. Courbin, A. Kester, I. Womack, and A. Chi, "Implementation of 3d printing technology in the field of prosthetics: Past, present, and future," vol. 16, no. 9. [Online]. Available: <https://www.ncbi.nlm.nih.gov/pmc/articles/PMC6540178/>
21. "An open source 3d-printed transitional hand prosthesis for children," vol. 28.
22. B.-H. Li and M.-C. Yang, "Improvement of thermal and mechanical properties of poly (l-lactic acid) with 4, 4-methylene diphenyl diisocyanate," vol. 17, no. 6, pp. 439–443, eprint: <https://onlinelibrary.wiley.com/doi/pdf/10.1002/pat.731>. [Online]. Available: <https://onlinelibrary.wiley.com/doi/abs/10.1002/pat.731>.
23. J. Barrios-Muriel, F. Romero-S´anchez, F. J. Alonso-S´anchez, and D. Rodriguez Salgado, "Advances in orthotic and prosthetic manufacturing: A technology review," vol. 13, no. 2, p. 295, number: 2 Publisher: Multidisciplinary Digital Publishing Institute. [Online]. Available: <https://www.mdpi.com/1996-1944/13/2/295>.
24. Exoskeleton developers must improve capabilities, cost, says maxon. Library Catalog: www.therobotreport.com. [Online]. Available: <https://www.therobotreport.com/exoskeleton-developers-mustrefine-capabilities-cost-says-maxon/>
25. eLEGS™ | berkeley robotics & human engineering laboratory. [Online]. Available: <https://bleex.me.berkeley.edu/research/exoskeleton/elegs/>
26. BLEEX | berkeley robotics & human engineering laboratory. [Online]. Available: <https://bleex.me.berkeley.edu/research/exoskeleton/bleex/>
27. "MINDWALKER: A brain controlled lower limbs exoskeleton for rehabilitation. potential applications to space."
28. E. Mikolajewska and D. Mikolajewska, "Exoskeletons in neurological diseases—current and potential future applications." [Online]. Available: <http://www.advances.umed.wroc.pl/en/article/2011/20/2/227/>
29. J. Li and H. Tanaka, "Rapid customization system for 3d-printed splint using programmable modeling technique – a practical approach," vol. 4, no. 1, p. 5. [Online]. Available: <https://doi.org/10.1186/s41205-018-0027-6> 17.
30. S. H. Teoh, Engineering Materials for Biomedical Applications. World Scientific, google-Books-ID: UMdpDQAAQBAJ.
31. N. Palastanga, Anatomy and Human Movement, 6th ed. Elsevier.
32. J. P. Hosking, U. S. Bhat, V. Dubowitz, and R. H. Edwards, "Measurements of muscle strength and performance in children with normal and diseased muscle." vol. 51, no. 12, pp. 957–963, publisher: BMJ Publishing Group Ltd Section: Research Article. [Online]. Available: <https://adc.bmj.com/content/51/12/957>.
33. G. R. H. Sandercock and D. D. Cohen, "Temporal trends in muscular fitness of english 10-year-olds 1998–2014: An allometric approach," vol. 22, no. 2, pp. 201–205. [Online]. Available: [https://www.jsams.org/article/S1440-2440\(18\)30438-9/abstract](https://www.jsams.org/article/S1440-2440(18)30438-9/abstract).
34. D. W. Abbot, D. V. V. Kallon, C. Anghel, and P. Dube, "Finite element analysis of 3d printed model via compression tests," vol. 35, pp. 164–173. [Online]. Available: <http://www.sciencedirect.com/science/article/pii/S2351978919307243>.
35. M. Shahzad, A. Kamran, M. Z. Siddiqui, and M. Farhan, "Mechanical characterization and FE modelling of a hyperelastic material," vol. 18, no. 5, pp. 918–924. [Online]. Available: <http://www.scielo.br/scielo.php?script=sciarttextpid = S1516 - 14392015000500918Ing = entlng = en>
36. R. W. Ogden and R. Hill, "Large deformation isotropic elasticity: on the correlation of theory and experiment for compressible rubberlike solids," vol. 328, no. 1575, pp. 567–583, publisher: Royal Society. [Online]. Available: <https://royalsocietypublishing.org/doi/10.1098/rspa.1972.0096>.
37. M. Ju, S. Mezghani, H. Jmal, R. Dupuis, and E. Aubry, "Parameter estimation of a hyperelastic constitutive model for the description of polyurethane foam in large deformation," vol. 32, no. 1, pp. 21–40. [Online]. Available: <http://journals.sagepub.com/doi/10.1177/026248931303200102>.
38. N. Kumar and V. V. Rao, "Hyperelastic mooney-rivlin model: Determination and physical interpretation of material constants," vol. 6, no. 1, p. 4.
39. D. Jiang and D. Smith, "MECHANICAL BEHAVIOR OF CARBON FIBER COMPOSITES PRODUCED WITH FUSED FILAMENT FABRICATION." 18.